Global Magnetohydrodynamic Simulation of a Comet : When a Comet Crosses a Heliospheric Sector Boundary

Yu Yi

Laboratory for Atmospheric and Space Physics,

University of Colorado, Boulder, CO 80309, U.S.A.

(Manuscript received 15 September 1994)

Abstract

A disconnection event (DE) of the cometary plasma tail is one of most spectacular phenomena observed in comets. Yet, for years it has remained one of the great unsolved problems in astronomy and space physics. The solar wind is thought to play a major role in the creation of comet plasma tail(type I) disconnection events. The goal of this paper is to present a mechanism that explains the disconnection event in terms of the local conditions at the comet.

Comparison of the solar wind conditions and 16 DEs in Halley's comet shows that DEs are associated primarily with crossings of the heliospheric sector boundary and apparently not with any other properties of the solar wind, such as a high speed stream[*Yi et al.*, 1994].

A 3-dimensional resistive magnetohydrodynamic simulation in this paper supports this association by showing that only front-side magnetic reconnection between the reversed interplanetary magnetic fields that exist when a comet crosses the heliospheric sector boundary [*Niedner and Brandt*, 1978] could reproduce the morphology of a DE, including ray formation [*Brandt*, 1982].

1. Introduction

1.1 Comets as Heliospheric Probes

The comets have been devine probes anticipating such dreadful events as the death of kings and generals, and the onset of wars, droughts and disease. Korea has distinguishable records in comet observation. She is one of a few civilizations who have recorded comet observation before Christ : China in about 1059 B.C., Greece in 467 B.C. Roma in 345 B.C., Babylonia in 234 B.C., and Korea in 49 B.C. [*Yeomans*, 1991]. Korean record has a reputation for its precise description. As an example, the record of 1759 comet Halley observation [*Nha*, 1982] is introduced in the modern astronomy book by Calder[1994]

A comet tail is composed of a plasma tail (type Ⅰ) and a dust tail (type Ⅱ). The plasma tail is straight and lies narrowly along the sun-comet line. The global magnetic structure of the plasma tail is seen in blue radiation emitted by fluorescing ions (princi-

pally CO^+) trapped on the field lines. The dust tail is spread out over a wide region and bent by the orbital motion of the comet. The dust tail is seen by reflected sunlight. The plasma tail appears bluish, the dust tail yellowish in color plate.

Before the space age, the comet was a unique probe of the heliosphere. *Biermann* [1951] first established the existence of the *solar wind* by studying the plasma tails of comets. He suggested that the acceleration of plasma structures within comet tails and the deviation of the plasma tail orientation from the sun-comet vector could be well explained by the dynamic aberration of a continuous radial flow of charged particles from the sun. *Alfvén* [1957] established the existence of the *interplanetary magnetic field* (IMF) frozen in the solar wind to explain the very high repulsive accelerations sometimes observed in type I tails (i.e. under disturbed conditions). The most successful Alfvén model of the cometary plasma tail has the IMF draped over the ionosphere of the comet with the cometary plasma trapped on the field lines. This formation of an induced magnetotail has become the very paradigm of a normal or quiet-time cometary plasma tail. Thus, the model developed historically gave a picture of the overall plasma structure of comets as produced by the solar wind. In particular, a comet's plasma tail is normally attached to the comet head. *Brandt et al.* [1972] used the astrometric measurement of the tail position to probe properties of the solar-wind velocity field for solar latitudes up to 40°-50°, an area that Ulysses probed directly for the first time in January 1994.

Occasionally the entire or partial plasma tail separates from the comet and drifts away anti-sunward and this is followed by a renewal of the plasma tail. The cyclic nature of this phenomenon, called a disconnection event (DE), was noted long ago. The first general scientific morphology of DEs was determined by *Barnard[1920]* at the turn of the century although he had little knowledge of the solar wind necessary to work toward a physical explanation.

DEs are not very rare. DEs occur over wide ranges in the heliospheric radius, heliospheric latitude, and the phases of the solar cycle. *Niedner* [1981] found 72 DEs of 29 comets during the years 1892-1976 from the literature and the archives of observatory photographs. Comet Morehouse 1908 had 9 DEs and comet Halley in 1910 showed 5 DEs. Recently, *Yi et al.* [1994] catalogued the 16 DEs of comet Halley in 1985-1986.

The basic picture of Alfvén's model was confirmed by the six spacecraft flybys of comets Giacobini/Zinner and Halley in 1985-1986. However, a mechanism for the disconnection event (DE) remained unresolved. The overall goal of this paper is to establish the mechanism for DEs.

The solar wind is thought to play a major role in the phenomena of comet plasma tail disconnection events (DEs). When we can reliably explain the link between comets and the solar wind, we will be able to explore the properties of the solar wind wherever there are comets even when cometary orbits extend to high solar latitudes. Once the physical connection between these phenomena has been established, the signatures of DEs can be used as a diagnostic of heliospheric processes.

1.2 Magnetic Reconnection

Magnetic reconnection is widely believed to play a crucial role in determining the topology of magnetic fields in cosmic plasmas and provides an effective way for the conversion of magnetic energy into kinetic energy. Applications of magnetic reconnection include the heliospheric current sheet, other planetary

magnetospheres, and many astrophysical plasmas where acceleration of high energy particles occurs by energy supply from prestored magnetic energy.

The concept of magnetic reconnection was originally proposed as an attempt to explain solar flares [*Giovanelli* 1946]. The hypothesis of magnetic reconnection was introduced as the process that spontaneously converts the stored magnetic energy to kinetic energy of the flares. The concept of magnetic reconnection was extened to the Earth's magnetosphere at the subsolar region of the magnetopause by *Dungey* [1961]. Later, magnetospheric substorms were interpreted in terms of magnetic reconnection [*McPherron et al.*, 1973; *Min et al.*, 1985]. This magnetic reconnection mechanism was applied to cometary ionospheres to explain the DE at the dayside [*Niedner and Brandt*, 1978] and tailside [*Ip*, 1985; *Russell et al.*, 1986].

2. Disconnection Events of Cometary Plasma Tail

2.1 Morphological Sequence of DE

The morphological sequence of DEs based on the collected image data is shown in Figure 1.

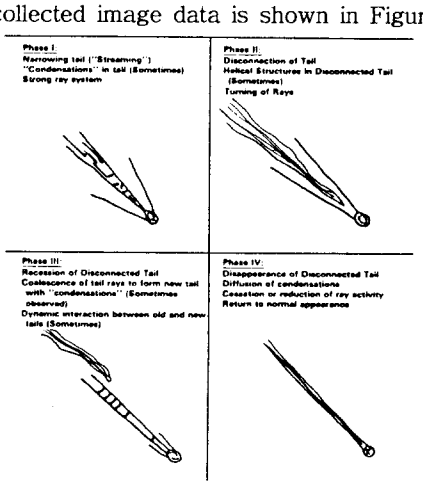

Fig. 1. A morphological sequence of DEs [*Brandt*, 1982].

Phase I : Strong folding rays appear. The neck of the old ion tail narrows between these rays.

Phase II : Rays are still folding. The old tail is disconnected. The disconnected tail sometimes shows helical structure.

Phase III : The disconnected tail is receding tailward. The tail rays coalesce to form a new tail, where condensations are sometimes found. Occasionally, there is a dynamic interaction between the old and new tail.

Phase IV : The disconnected tail disappears. Condensations diffuse into the new tail, and tail activity is ceased or reduced. Everything returns to a normal appearance.

One ideally symmetric ray folding case on the second phase is shown in Figure 2. Comet Tago-Sato-Kosaka 1969 IX was seen progected on a plane nearly perpendicular to its orbit.

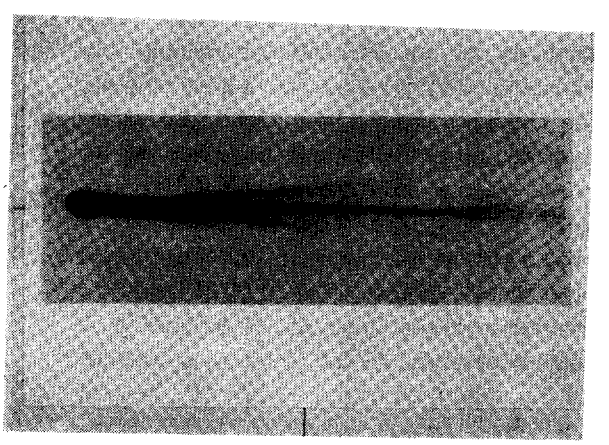

Fig. 2. An example of the disconnection of plasma tail with symmetric folding rays in the second phase of Figure. A photograph of Comet Tago-Sato-Kosaka 1969 IX, seen projected on a plane nearly perpendicular to its orbit on 28 December 1969, was taken by *Miller* [1979]

2.2 Suggested Ideas for DE

Barnard [1920] described the general scientific morphology of DEs but lacked the knowledge of the solar wind necessary to work toward a physical explanation. *Niedner and Brandt* [1978] made the first attempt to explain DEs by invoking the solar wind conditions. Since then, many theories have been suggested as explanations of DEs, but a fully self-consistent 3-dimensional model for DEs did not exist. The current competitive theories can be grouped into three classes based on the triggering mechanisms.

(1) *Ion Production Effects* : If the ion production rate were drastically reduced on a short time scale less than an hour, the ionosphere of the comet could shrink temporarily and allow the magnetic field lines to slip away. The change of ionization rate in the comet could be strongly influenced by a change in the solar UV radiation or in the density of neutral out of which the ions are created [*Wurm and Mammano*, 1972].

(2) *Pressure Effects* : A large dynamic pressure increase in the solar wind could compress the comet's ionosphere and either free the magnetic field lines or excite various instabilities (e.g., Rayleigh-Taylor) in the tail. If this is the correct mechanism, one would expect DEs to be associated withe high-speed streams [*Ip and Mendis, 1978*; *Jockers*, 1985], high density regions, or flare-generated interplanetary shocks.

(3) *Magnetic Reconnection Effect* : There are two versions of the magnetic reconnection model. One suggests that sunward magnetic reconnection occurs as the comet crosses the IMF sector boundary-the heliospheric current sheet(HCS) [*Niedner and Brandt*, 1978]. But because a larger percentage of sector boundaries are correlated with the leading edges of high speed streams, it is sometimes difficult to distinguish between pressure effects and front side reconnection during magnetic sector boundary crossings. The other possibility is that the magnetic reconnection occurs on the tail side [*Ip*, 1985; *Russell et al.*, 1986]. According to *Russell et al.* [1986], the tail side reconnection might be triggered by either an interplanetary corotation shock or a high-speed stream (a decrease in the Alfvén Mach number), but *not* by an IMF sector boundary.

3. Disconnection Events of Comet P/Halley

3.1 Associations of DEs with the Heliospheric Sector Boundaries

Yi et al. [1994] compared cometary and solar wind data for the purpose of determining the solar wind conditions associated with comet plasma tail disconnection events (DEs).

In situ solar wind measurements from IMP-8, ICE, and PVO were used to construct the variation of solar wind speed, density, and dynamic pressure during this interval. Data from these same spacecraft plus Vega-1 were used to determine the time of 48 current sheet crossings. The cometary data are from *The International Hally Watch Atlas of Large-Scale Phenomena* [*Brandt, Niedner, and Rahe*, 1992]. The Large Scale Phenomenon Network (LSPN) of the International Halley Watch (IHW) collected and archived most of the wide-field images of comet Halley taken during the time period from November 1985 to July 1986. This database of photographs includes two Korean photographs, one by Nha, I.-S. and Kim, H.-I., and 16 DEs in Halley's comet, chosen based on the Atlas, shows that DEs are associated primarily with crossings of the heliospheric sector boundaries and apparently not with any other properties of the solar wind such as a high speed stream.

3.2. Spacecraft Observations

Front-side reconnection model is based on the assumption that front-side reconnection of the captured IMF at a heliospheric sector boundary crossing causes the DE [*Niedner and Brandt*, 1978]. There were some *in situ* measurements by the Vega spacecraft near the time of the comet Halley DE on 8.4 March 1986 [*Verigin et al.*, 1987] supporting these models. The Vega-1 spacecraft passed in front of the comet on 6 March 1986, and Vega -2 passed in front on 9 March 1986. An heliospheric sector boundary was detected by Vega-1 on 7.9 March 1986. Combining measurements of both Vega-1 and Vega-2, *Niedner and Schwingenshun* [1987] Showed that a reversal of the cometary magnetic field occurred between the two encounters.

The overall topology of the magnetic field around closest approach of Vega-1, deduced from the measurements of the magnetic field direction along the Vega-1 trajectory and in the region where the burst of accelerated ions was observed, was an expected feature of the front-side magnetic field reconnection model [*Verigin et al.*, 1987]. When *McKenna-Lawlor et al.* [1980] investigated the records of instruments aboard Giotto and Vega-1, they reasoned that the merging of magnetic field lines of opposite polarity in front of the comet was responsible for acceleration cometary particles which were in the cometosheath.

4. MHD simulation of the Interaction between Comet and Solar Wind

4.1 History of MHD Simulation

For the global cometary plasma simulation, many magnetohydynamic studies have been performed in two dimension [*Schmidt and Wegmann*, 1980; *Ogino et al.*, 1986], and three dimensions [*Wegmann et al.*, 1987; *Ogino et al.* 1988; *Schmidt-Voigt*, 1989; *Russell et al.*, 1991; *Yi and Brandt*, 1992]. Most of the earlier works were focused on the steady state structures of comets interaction with various solar wind conditions. MHD simulations have achieved quite successful results in providing a global view of the whole interaction processes, which describes the plasma density distribution, plasma pressure (temperature), the plasma flow and the magnetic field structure. But, dynamically changing features were not deeply investigated.

Simulations of dynamic responses to solar wind variations have been tried only by *Ogino et al.* [1986] in two dimension and *Schmidt-Voigt* [1989] in three dimension. *Ogino et al.* [1986] simulated the interaction of solar wind with outflowing plasma from a comet when the IMF orientation is reversed, and found that dayside magnetic reconnection occurs at the subsolar point. A large-scale disturbance occurs throughout the entire tail region and this disturbance propagates down the tail. *Schmidt-Voigt* [1989] tested two cases of reversal of the IMF and 90° tangential rotational discontinuity of the IMF. He reported that there was no front-side magnetic reconnection in his interpretation of the magnetic field vector plot and that he could see only tiny plasma condensations in the tail in the later case.

The 2-dimensional MHD simulation is good enough to show the magnetic field configuration in the plane of the IMF including the coma. However, it is not realistic from the viewpoint that many of the IMF flux ropes can avoid the nucleus by motion in the third dimension. So, tail-side magnetic reconnection tends to be forced by the 2-dimensional simulation.

The field of global 3-dimensional MHD simulations has developed the ability to test the causalities and the processes of interaction between the solar wind and comets in a real situation in response to changes in the solar wind.

A global time-dependent resistive compressible 3-dimensional MHD simulation code with non-uniform grids has been written. In the plasma structure of a comet interacting with the solar wind, there are many scale lengths - from the contact surface distance, to the distance of the shock from the comet nucleus, to the length of the whole plasma tail. These correspond to $4,000km$, $1\times10^{6}km$ and $15\times10^{6}km$, respectively in comet Halley. Therefore, to fit the program into the available computers and to match the physical scales of the problem, a variable grid spacing was used.

4.2. Numerical Model

The resistive compressible MHD equations with plasma source term A outflowing with velocity **W** can be written for the time-dependent MHD simulation as follows :

$$\mathbf{J} = \frac{1}{\mu_0}(\nabla\times\mathbf{B}) \tag{1}$$

$$\frac{\partial \rho}{\partial t} = -\nabla\cdot(\mathbf{V}\rho)+A \tag{2}$$

$$\frac{\partial \mathbf{V}}{\partial t} = -(\mathbf{V}\cdot\nabla)\mathbf{V} - \frac{1}{\rho}\nabla P+\frac{1}{\rho}\mathbf{J}\times\mathbf{B} + A\frac{(\mathbf{W}-\mathbf{V})}{\rho} \tag{3}$$

$$\frac{\partial P}{\partial t} = -(\mathbf{V}\cdot\nabla)P - \gamma P\nabla\cdot\mathbf{V}+\frac{\gamma-1}{2}\times A(\mathbf{W}-\mathbf{V})^2+\eta(\gamma-1)\mathbf{J}^2 \tag{4}$$

$$\frac{\partial \mathbf{B}}{\partial t} = \nabla\times(\mathbf{V}\times\mathbf{B})+\eta\nabla^2\mathbf{B} \tag{5}$$

Where ρ, **V**, P, **B**, and η are the plasma mass density, the plasma flow velocity, the plasma pressure, the magnotic field, and the resisitivity, respectively. The adiabatic constant γ of this 3-dimensional calculation is taken to be 5/3.

The MHD equations are solved as an initial value problem by the two-step Lax-Wendroff method which is a very effective algorithm for solving the equations that govern inviscid, compresssible flow.

The coordinate system used in this 3-dimensional MHD simulation is shown in Figure 3 in CSE (Comet-centered Solar Ecliptic) coordinates. A full 3-dimensional box was used rather than the quarter box ($y>0$, $z>0$) with the appropriate mirror boundary conditions at $y=0$ and $z=0$, because simulation of the 90° tangential rotation and the inclined IMF (not in this paper) are not possible with quarter box simulations.

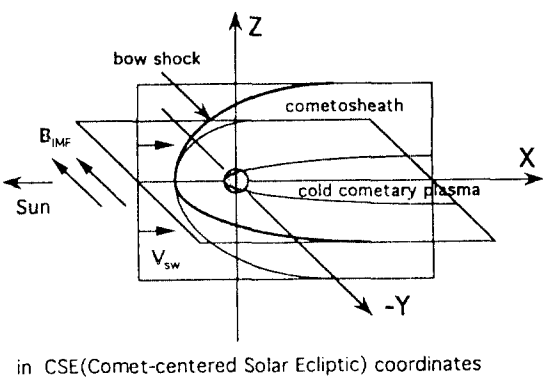

Fig. 3. Coordinate system in CSE (Comet-centered Solar Ecliptic) coordinates used in this 3-dimensional MHD simulation

The non-uniform grid was used instead of the uniform grid used by *Ogino et al.*, [1988] in order to optimize between the CPU time and memory and coverage of the tail. The grid points $(N_x, N_y, N_z) = (75, 46, 46)$ were set up. The other 3-dimensional simulation for a test of IMF tangential rotation effects have used (33, 17, 17) [*Schmidt-Voigt*, 1989]. The mesh sizes are varied for the differential grid code,

Δx = 20,000~200,000 km, Δy = 20,000~100,000 km, Δz=20,000~10,000 km. The time step was selected as Δt=40 sec $< \frac{1}{4}\frac{\Delta x_{min}}{v_{su}}$ in order to assure numerical stability.

The spatial extent of the numerical grid is $-1.2 \le X \le 8.0$, $-1.2 \le Y \le 1.2$, $-1.2 \le Z \le 1.2$ in unit of 10^6 km and the comet was placed at the origin of the CSE coordinates.

One serious problem in MHD calculations is to keep the condition $\nabla \cdot \mathbf{B}=0$ reasonably satisfied despite the numerical roundoff errors. If code uses centered difference one direction do not depend on those in other directions, and $\nabla \cdot \mathbf{B}=0$ is well satisfied without a cometary ion source.

4.3. Steady States

The parameters of the solar wind plasma and IMF are : v_{sw}=350 km sec^{-1}, n_{sw}=15 cm^{-3}, $T_{sw}=2\times10^5$ °K ($P_{sw}=10^{11}$ dyn cm^{-2}) and $B_{IMF}=B_y$=20 nT, which are the typical average values of the solar wind plasma and IMF at r=0.7 AU. I have used somewhat higher values of solar wind parameters than others who used the solar wind parameters at 1.0 AU since these are the conditions where most of the DEs occur.

Here, we are interested in cometary plasma rather than neutral gas, and so I consider the neutral gas only as a source of comet plasma. Photoionization is assumed as the only ionization mechanism in this simulation. The comet's is modeled by the cometary plasma source A outflowing with velocity **W** as follows :

$$A = \frac{m_i Q_o}{4\pi r_i r^2} e^{-\frac{r}{r_i}} \mathbf{f}(\theta) \quad (6)$$

$$\mathbf{W} = v_c \mathbf{r} \quad (7)$$

Where m_i in the mass of cometary ions, Q_o is the gas production rate, r_i is the ionization distance, $f(\theta)$ is an axis-symmetric model of the ion source term and v_c is the radial velocity.

The parameters of ion production for comet Halley are as follows : the gas production rate $Q_o=1.0\times10^{30}$ sec^{-1}; the ionization rate $\sigma=1.0\times10^{-6}$ sec^{-1}; the radial flow velocity $v_c=1.0$ km sec^{-1}; the ionization distance $r_i=\frac{v_c}{\sigma}=1.0\times10^6$ km; and the effective mass of the ion normalized to the proton mass $m_i=18\ m_p$. Constant resistivity model $\eta=\eta_o$, where η_o=0.001, was used.

The solar wind with the velocity v_{sw} in the x-direction accompanied by a uniform IMF frozen in the y-direction flows into the simulation box through the boundary YZ-plane at the left side and interacts with the cometary outflowing plasma. The free boundary conditions where the spatial derivatives of the physical quantities are zero are applied to the side boundaries and the tail boundary, so the plasma can leave and enter the simulation box freely. However, the plasma pressure was kept $P=P_{sw}$ at all boundaries to assure numerical stability.

The simulation started with the initial conditions where a uniform solar wind with an IMF filled the whole simulation box, because it keeps the pressure balance better in the tail. The simulation ran it until a quasi-steady state was reached. This required about 10.7 hours in real time, equivalent to 960 time steps. After this time, the tail was getting longer in the low density downstream region, while the high density region, up to x=300,000 km, did not reveal any noticeable changes. This agrees with the simulations done by *Ogino et al.* [1988] and *Russell et al.* [1991].

The magnetic Reynold's number, the ratio of the magnetic diffusion time to the Alfvén transit time, is $Rm=\frac{\Delta_{xyz}}{\eta} > 500$, where Δx is the mesh size and v_A is the local Alfvén velocity.

The configurations of captured magnetic

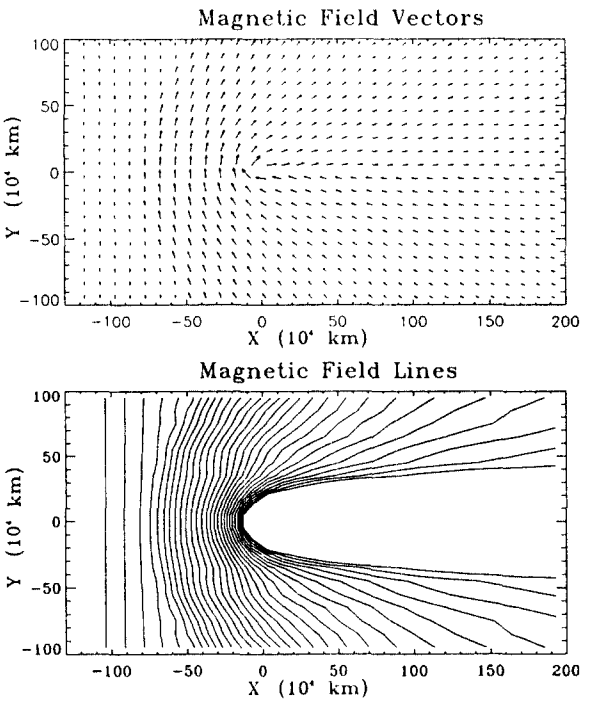

Fig. 4. Configurations of magnetic field vectors (a) and magnetic field lines (b) in the XY-plane.

fields in the XY-plane ($z=0$) are shown in the form of vector field and field lines in Figure 4. The field lines in Figure 4 (b) follow each other in time intervals of approximately 7 minutes.

Figure 5 shows the profiles of density ρ, plasma pressure P, plasma temperature T, solar wind velocity V_x, and magnetic field B_y along the sun-comet line. As the solar wind interacts with the cometary plasma, a bow shock forms. The shock is indicated by the gradients in the plasma pressure and magnetic field and velocity magnitude and direction changes in the velocity flow pattern and IMF. The bow shock is about $75\times10^4 km$ from the comet along the sun-comet line.

4. 4. When a Comet Crosses a Heliospheric Sector Boundary : IMF Reversal

The reason every DE is somewhat different in specific features is that a DE is triggerred by the mixed characteristics of the solar wind. Also, the shape (column density configuration)

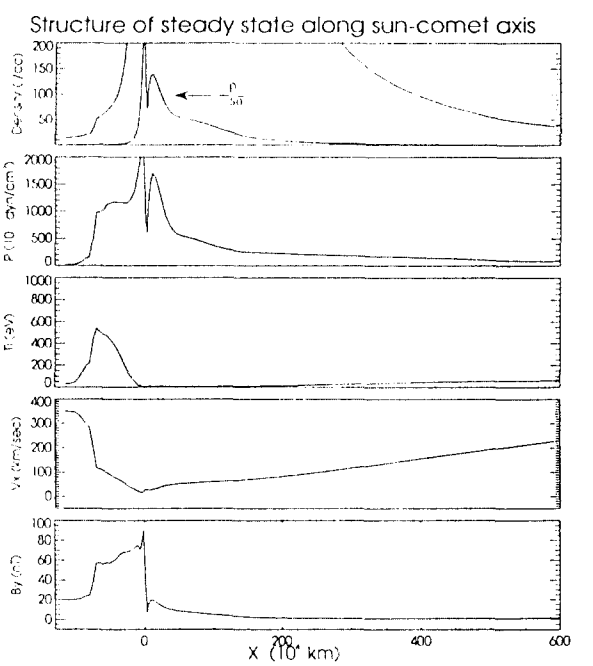

Fig. 5. Profiles of density ρ, plasma pressure P, plasma temperature T, solar wind velocity V_x, magnetic field B_y along the sun-comet line.

of a 3-dimensional structure is dependent on the viewing angle. However, as described in the section 2.1, most of DEs have shown many of the same features such as rays folding before the disconnection of the old tail. Therefore, there might be one characteristic in the solar wind which could cause these DE similarities. With the help of the explicit time-dependent 3-dimensional MHD code, we can simulate the comet responses to the idealized (modeled) solar wind variations of each parameter separately to see how each one influences the comet.

In order to test the front-side magnetic reconnection model of *Niedner and Brandt* [1978], the IMF direction was reversed (180° tangential rotation) with the same magnitude from steady state solar wind condition, from $B\hat{y}$ to $-B\hat{y}$, as an imitation of the typical heliospheic sector boundary. Time sequences of configurations of many quantities influenced by this IMF reversal are displayed in figures following. The time displayed on the each panel is the time after the field reversal.

In Figure 6 (ion density in the XY-plane), the symmetric new ion rays appeared about 4.8 hours after the reversed IMF enters the simulation box and were folding toward the old central plasma tail. The narrowing of the old tail between rays was seen as shown in the morphological scheme of DE evolution in Figure 1(a). After 7.5 hours, the old tail was disconnected between the folding rays as drawn in Figure 1(b). The disconnected tail was receding downstream at 2.0×10^{6}*km* at t= 11.5 hours. It receded until it passed out of the tail side simulation boundary.

The rays were formed along the draped magnetic neutral sheet, shown in Figure 12. The measured ray folding rate of comet Kobayashi-Berger-Milon 1975 IX was $\sim3°hr^{-1}$ within 10° [*Brandt*, 1982]. Rays are discernable till 3°. The ray folding time scale was ~15 hours from 60° to 5° for most of the studied comets by *Wurm and Mammano* [1972].

In the simulation, the ray folding rate was about $10.8°hr^{-1}$ from 45° at t=4.8 hours to 15° at t=7.5 hours and $2.15°\ hr^{-1}$ from 15° at t=

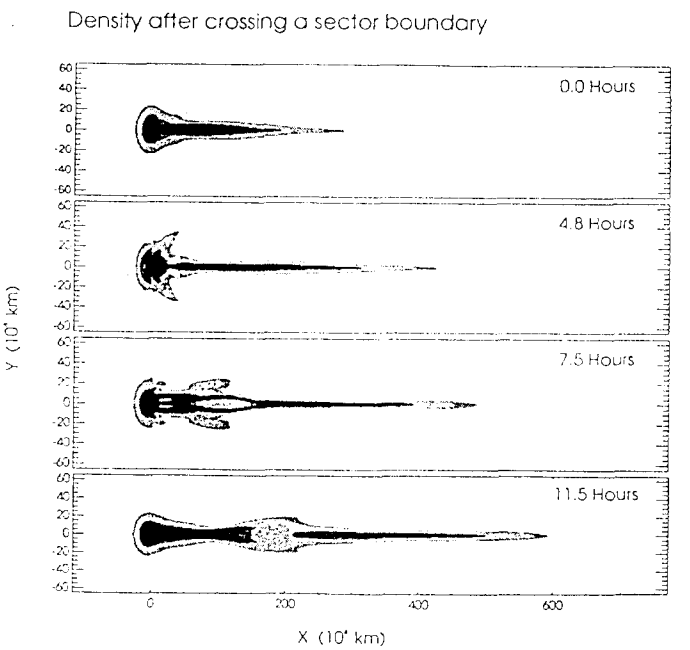

Fig. 6. Configuration of ion density in the XY-plane after IMF direction is reversed.

7.5 hours to 6.4° at t=11.5 hours. We can estimate the folding time between 60° and 5° at less than 10 hours. Folding rays were not distinguished near the tail axis. The calculated and observed folding rates are in satisfactory agreement.

In Figure 7 (ion density in the XZ-plnae where the old IMF direction is coming out and the new reversed IMF is going into the paper), we cannot see the folding rays as distinctive as in the XY-plane. However, at t=4.8 hours we can see that the ions in the ionosphere of the comet were stripped out of the XZ-plane (less dense than the steady state). We can see the disconnected old tail between the rays clearly 7.5 hours later. At 11.5 hours, the folding rays in the high density region became a new tail. The third panel image is very similar to the photograph in Figure 2, where the given geometical conditions are same, even though the folding rays are not so long as in the real image.

In this MHD simulation, the asymmdtric configurations of density plots in XY-plane and XZ-plane were seen in the steady state because the magnetic stresses of the draped IMF push the plasma towards XZ-plane. The hydrodynamic model without the IMF should be axis-symmetric with respect to the sun-comet line. Ion column density plots look very similar to ion density plot XY- and XZ planes.

In Figure 8 (plasma pressure in the XY-plane), the high pressure rays are folding, as seen in the density configuration along the draped heliospheric current sheet, and the old tail is disconnected between the folding rays. The high pressure rays appear at t=4.8 hours. Behind this pressure barrier, the tail is reduced. Eventually, the old tail was disconnected between the folding rays at t=7.5 hours. At t=11.5 hours, the symmetric folding rays coalesced into a new tail near the coma, but farther down in the tail the ray was still folding around the disconnected tail. This process can also be interpreted with the revised ionization effect model of a DE by

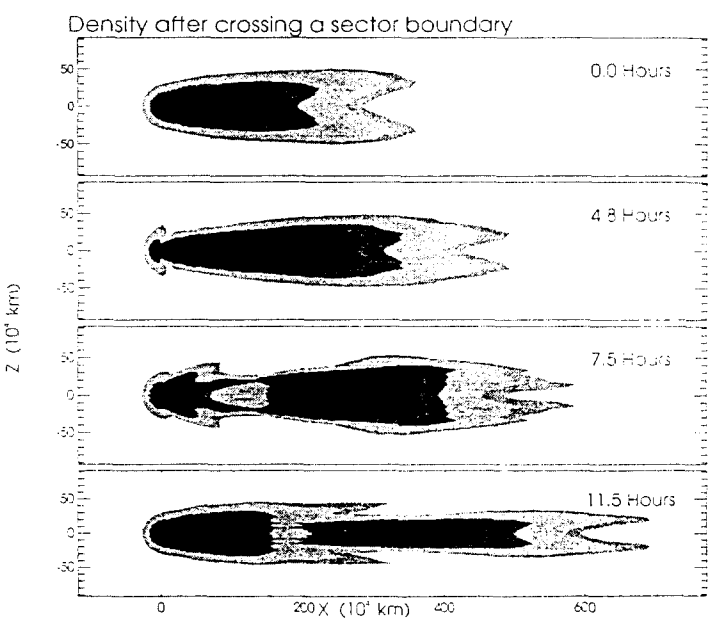

Fig. 7. Configuration of ion density in the XZ-plane after IMF direction is reversed.

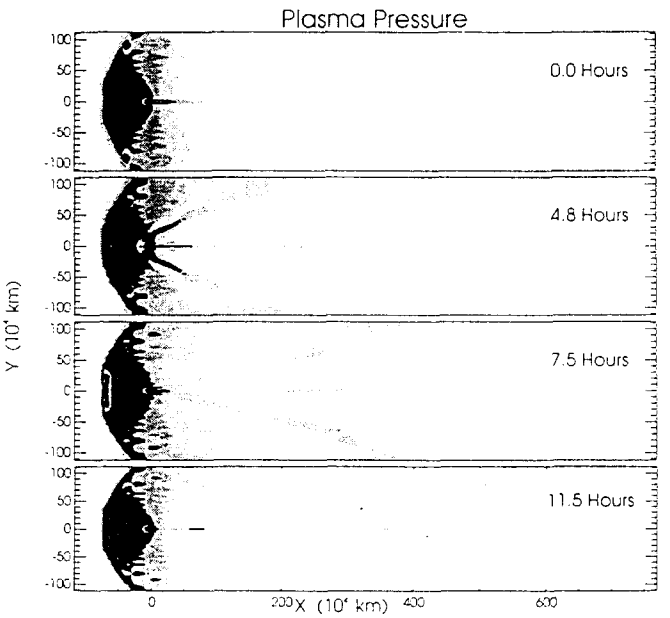

Fig. 8. Configuration of plasma pressure in the XY-plane after IMF direction is reversed.

Wurm and Mamanno [1972]. They suggested that the exhaustion of the ion source causes the disconnection of the old tail. It can be rephrased that the exhaustion of ion supply to the tail contributes to the plasma disconnection when the newly-formed ion rays are folding.

The captured IMF vectors is shown in Figure 9(a). The magnitude of the magnetic field vectors was small in the neutral sheet boundary where magnetic field directions are reversed. The x-type magnetic reconnection in the day-side cometosheath occurs was seen in Figure 9(b), when it was drawn in the form of magnetic field lines draped around the comet. The field lines in Figure 9(b) follow each other in time intervals of approximately 7 minutes. When the reversed IMF reaches the high magnetic field density region of draped field lines, the dayside magnetic reconnection begins to occur at the subsolar point and the previously captured IMF lines are stripped from the dayside. The front-side magnetic reconnection is shown only in the XY-plane ($z=0$), however, the similar configuration is formed in other XY-planes ($z\neq0$). The x-type neutral point in 3-dimensions actually forms a line in the XZ-plane, and this topology may account for some plasma features in comet. In a 3-dimensional configuration, the front-side magnetic reconnection is occurring all along the current sheet in the cometosheath where the deceleration is strong.

Figure 10 presents the evolution of the configuration of magnetic field lines in the XY-plane showing the front-side magnetic reconnection after the IMF direction is reversed. Figure 11 compares the velocity field vectors in steady state and when the front-side magnetic reconnection is going on, we can see that flows are deflected along the IMF lines where front-side magnetic reconnection is going on. Figure 10 and Figure 11 are the expected morphologies of front-side magnetic field systems. It also changes the flow vector

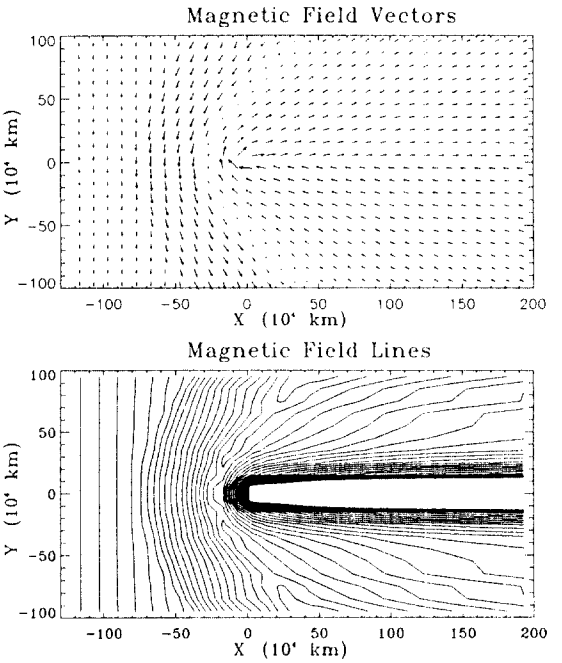

Fig. 9. Configuration of magnetic field vectors in the XY-plane after IMF direction is reversed.

field of plasma frozen in the magnetic field.

In Figure 12 (magnetic pressure in the XY-plane), the white band of $|\mathbf{B}| < 4$ nT shows movement of the draped IMF sector boundary where the front-side magnetic reconnection process is going on. The brighter gray region marks the higher magnetic pressure in the original IMF direction of the positive B_y

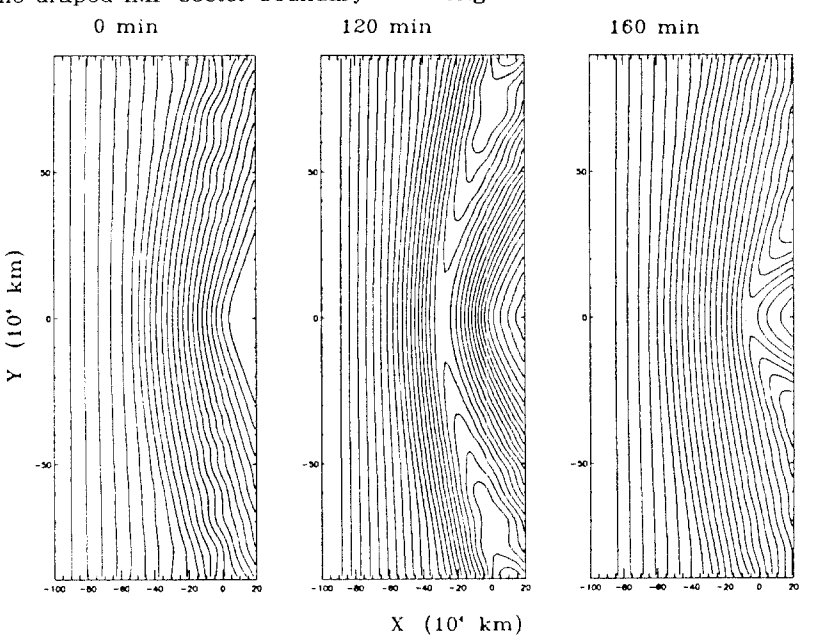

Fig. 10. Configuration of magnetic field lines in the XY-plane after IMF direction is reversed.

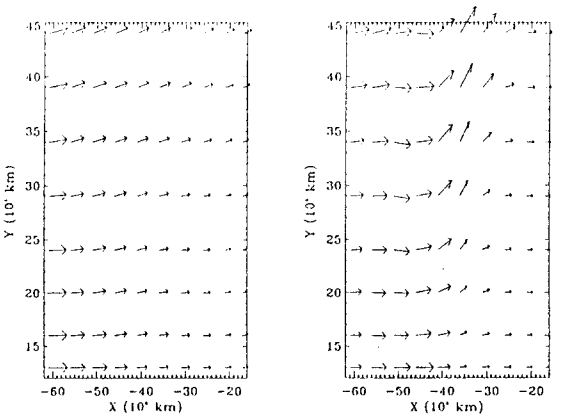

Fig. 11. Configuration of flow vector field in the XY-plane after IMF direction is reversed; (a) is the steady state and (b) is the situation after 2 hours.

component. The darker black region marks the higher magnetic pressure in the reversed IMF direction of the negative B_y component.

In Figure 13 (magnetic pressure in the XZ-plane), the white band of $|\mathbf{B}| < 7$ nT shows two regions. One is the cometary neutral sheet of the old plasma tail, and the other one, approaching from the sides, is the draped IMF sector boundary, where the front-side magnetic reconnection process is going on. The disconnected tail has the old IMF polarity, and the newly forming tail following the draped IMF sector boundary has the new reversed IMF polarity.

4.5 Simulated Spacecraft Observations of a Rendezvous Misson

It is possible to simulate expected spacecraft observations in some future comet rendezvous mission at the time of ground observations of a DE. It could help us to verify the details of the triggering mechanism of a DE. The spacecraft was assumed to be located at a fixed point in CSE coordinates (x=30,000 km, y=200,000 km and z=10,000 km in comet Halley class) to simplify the data collecting process, even though the rendezvous mission

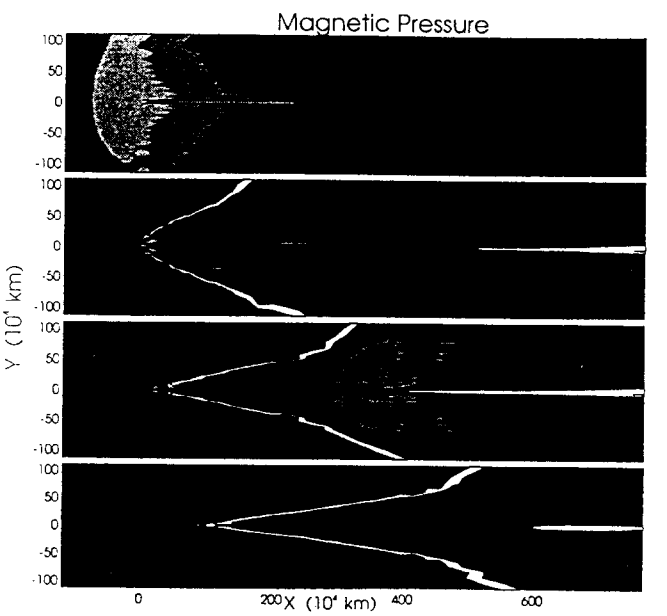

Fig. 12. Configuration of magnetic pressure in the XY-plane after IMF direction is reversed.

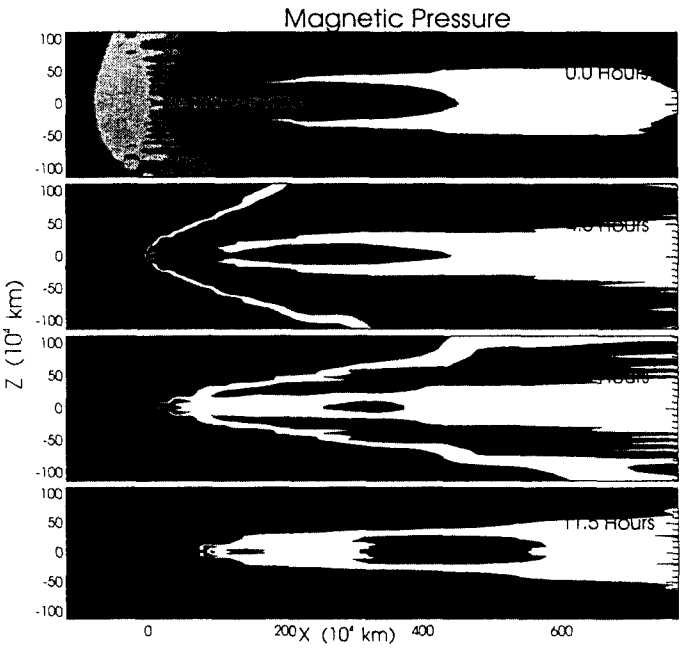

Fig. 13. Configuration of magnetic pressure in the XZ-plane after IMF direction is reversed.

would orbit around the comet. Figure 14 shows the time-dependent variation of plasma parameters after the IMF reversal (comet's heliospheric sector boundary crossing).

Around the neutral sheet where the magnetic reconnection is going on (B_y changes sign), the plasma temperature goes up to 200 eV as observed by Vega-1 [*Verigin et al.*, 1987] and the V_y increases due to the plasma acceleration, $(\mathbf{J}\times\mathbf{B})\cdot\mathbf{V}$, produced by the magnetic reconnection between the reversed polarities of the IMF. The pitch angle (angle between the magnetic fied and ion flow directions) shows a sudden 180° change. These happen about at t=3 hours after the IMF reversal at the inflowing boundary of the simulation box. The disconnected tail was seen 7.5 hours after the IMF reversal. Thus, we can observe from the ground the disconnected tail 4.5 hours after the spacecraft detects the features (described above) in the plasma.

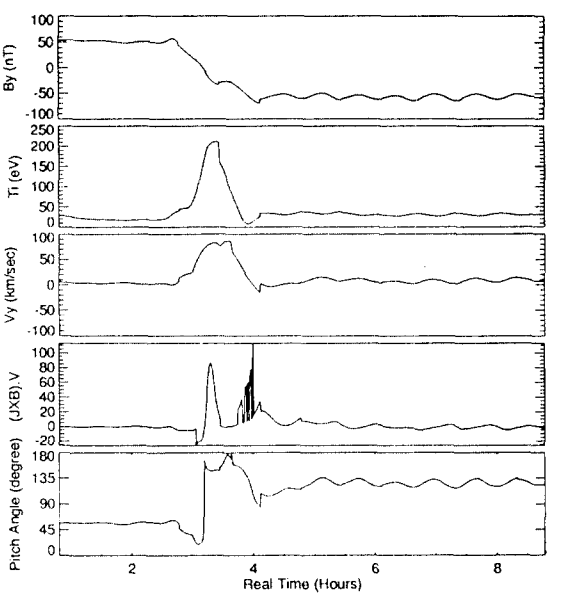

Fig. 14. Variation of plasma parameters as a function of evolutionary time after the IMF reversal, observed by spacecraft at the fixed point in CSE coordinates (x=30,000 km, y=200,000 km and z=10,000 km).

4.6 Comparisons and Discussions

New features of the front-side magnetic reconnection driven by the IMF reversal are these :

1) The front-side magnetic reconnection field morphology is obviously shown.

2) The plasma heating energy (plasma temperature increase) was transformed from the magnetic field energy by magnetic reconnection. The plasma pressure increase along the line (plane in 3-dimensional configuration, we can see it in XY-plane and XZ-plane) of the neutral sheet.

3) It is discovered that the long ray formation occurs along the neutral sheet line [*Ness and Donn*, 1965] by the front-side magnetic reconnection, and the ray was being folded toward the old neutral sheet.

4) The original comet tail with old magnetic polarity is disconnected when the neutral sheet has just passed the coma. The folding rays are forming a new tail with new magnetic polarity and new tail was growing.

5) Most importantly, we could observe the disconnected plasma tail (as seen in the photographic image in Figure 2) flowing tailward while wrapped by the rays along the neutral sheet.

The first three features are strong evidence of the front-side magnetic reconnection and the last two were observed features in DE process (*Brandt*, 1982). The plasma pressure increase in 3-dimensions along the whole neutral sheet draped at the cometosheath, where the magnetic reconnection is driven by the deceleration, means that front-side magnetic reconnections is going on along the whole neutral sheet as well as the in the XY-plane ($z=0$)

Schmidt-Voigt [1989] reported that he could not see any reconnection occur and that the structure of the comet was not changed by the IMF reversal with his ideal MHD model. However, when the magnitude of the magnetic field vectors was drawn in the form of magnetic field lines draped around the comet, the x-type magnetic reconnection in the day-side cometosheath was seen clearly. The decrease in magnitude of the magnetic field vectors means that the magnetic field energy was converted to other forms like plasma heating and plasma acceleration. The strong pressure barrier produced by the magnetic reconnection hinders the plasma supply to the near tail and leads to disconnection of the old plasma tail, called *Umbrella Effect* [*Ness and Donn*, 1965]. This ray formation and the old tail disconnection between the newly formed rays are observed features of DE evolution described by *Brandt* [1982].

It is shown that an IMF reversal could trigger the folding rays (the fan-shaped folding rays in column density plot) observed during the process of a DE. The many observed features of comet Halley DEs favor the front-side magnetic reconnection model of heliospheric sector boundary crossing. Only the IMF reversal case satisfies the morphological sequences of a DE [*Brandt*, 1982] and it confirms the front-side magnetic reconnection model [*Niedner and Brandt*, 1978].

5. Conclusion

Before the space era, comets were the only available probes of the heliospheric structure. The astronomical observations of cometary plasma tails have led to the postulation of the continuous corpuscular stream [*Biermann*, 1951], called the *solar wind* [*Porker*, 1958], to the introduction of the *interplanetary magnetic field* (IMF) frozen in the heliosphere [*Alfvén*, 1957], and to the determination of the solar wind velocity field in the heliosphere [*Brandt et al.*, 1972]. The solar corpuscular radiation and the IMF were confirmed by spacecraft in

the 1960s and the Ulysses Mission has detected the high speed solar wind in high solar latitudes.

The solar wind plays a major role in the plasma tail disconnection event (DE), which is characterized by the plasma tail being uprooted from the comet head and convected downstream in the solar wind while being replaced by a new tail constructed from folding rays. Therefore, once the physical connection between the DE and the solar wind conditions has been established, the DE signature can be used as another diagnostic of heliospheric structures. The DE was one of the problems debated for more than a decade in astronomy and space physics before the results of this research.

When a comet crossed a sector boundary, the heliospheric current sheet was draped in the cometosheath and the front-side magnetic reconnection occurred with x-type neutral points at the subsolar point as the current sheet approachig the nucleus. The Change of magnetic field configuration due to the front-side magnetic reconnection deflected the ion flow along the current sheet. This deflected flow to the side made symmetrical rays. It hindered the pick-up ions from being supplied to the central tail. It continued until the current sheet passed the nucleus and the old plasma tail was disconnected between the folding rays, as seen in Figure 2. This process can be called Umbrella Effect : The squeezed current sheet within the sub-Alfvénic region of cometosheath, where the front-side magnetic reconnection is going on, plays a role similar to the opening of an umbrella, which prevents rain flow under the umbrella. Then the new folding rays coalesced to replace the old tail. The global morphology of the DE does not depend on the resistivity model. In the process of magnetic reconnection, the energy input to the plasma was supplied by conversion from magnetic energy by magnetic reconnection. This kind of hot ion burst where magnetic polarities were changed was first observed by Vega-1 on the comet Halley [*Verigin et al.*, 1987]. This hot ion burst in the dayside might trigger an ionization avalanche which causes the coma brightening.

Any future comet rendezvous mission such as Rosetta mission by European Space Agency with the full support of ground-based observations for that period will make it possible to explore the regions where the plasma tail connects to and disconnects from the ionosphere in order to investigate the precise conditions under which the DEs are triggered. Jets from the magnetic reconnection in the head during the onset stage of DE may be observed with very high spatial resolution images and spectrophotometry by this kind of mission. Simulated signatures of the plasma parameters can be also very useful to verify the cause and the process of DEs.

In conclusion, the front-side magnetic reconnection mechanism of a DE [*Niedner and Brandt*, 1978] is confirmed by the strong association of 16 comet Halley DEs with sector boundaries, and a global 3-dimensional MHD simulation shows that the front-side magnetic reconnection is the major cause of a DE when the comet crosses the sector boundary.

Acknowledgements

It is a pleasure to express my thanks to Dr. John C. Brandt in Laboratory for Atmospheric and Space Physics, University of Colorado at Boulder for his lessons about cometary and heliospheric physics. My appreciation also goes to Professor Tatsuki Ogino in Nagoya University and Professor Raymond J. Walker of UCLA who helped me to start the numerical simulation.

References

Alfvén, H., On the Theory of Comet Tails, *Tellus*, 9, 92-96, 1957.

Barnard, E. E., On Comet 1919b and on the Rejection of a Comets Tail, *Astrophys. J.*, 51, 102-106, 1920.

Biermann, L., Kometenschweife und Solar Korpuskularstrohlung, *Zs. F. Astrophys.*, 29, 279-286, 1951.

Brandt, J. C., Observations and Dynamics of plasma tails, in *Comets*, ed. L.L. Wilkening, University of Arizona, Tucson, p. 519, 1982.

Brandt, J. C., Roosen, R.G. and Harrington, R.S., Interplanetary Gas XVⅢ. An Astrometric Determination of solar wind velocities from orientations of ionic comet tails, *Astrophys.* J., 177, 277-284, 1972.

Brandt, J. C., Niedner, M.B., Jr., Rahe, J., in *The International Halley Watch Atlas of Large-Scale Phenomena*, LASP, U. of Colorado, Boulder, 1992.

Calder, N., in *Comets: Speculation and Discovery*, Dover, New York, p. 15, 1994.

Dungey, J. W., Interplanetary magnetic field and the auroral zones, *Phys. Rev. Lett.*, 6, 47, 1961.

Giovanelli, R. G., A Theory of Chromospheric Flares, *Nature*, 158, 81, 1946

Ip, W.-H., Solar wind interaction with neutral atmospheres, in *Proc. ESA Workshop on Future Missions in Solar, Heliospheric and Space Plasma Physics*, ESA SP-235, 65-82, 1985.

Ip, W.-H., and Mendis, D.A., The Flute Instabilty as the Trigger Mechanism for Disruption of Cometary Plasma Tails, *Astrophys. J.*, 223, 671, 1978.

Jockers. K., The ion tail of comet Kohoutek 1973 XⅡ during 17 days of solar wind gusts, *Astron. Astrophys. Suppl.*, 62, 791-838, 1985.

Mckenna-Lawlor, S., Daly, p., Kirsch, E., Wilken, B., O'Sullivan, D., Thompson, A., Kecskemety, K., Somogyi, A., and Coates, A., *In situ* energetic particle observations at comet Halley recorded by instrumentation aboard the Giotto and Vega 1 missions, *Ann. Astrophysicae*, 7. 121, 1989.

McPherron, R.L., Russell, C.T., and Aubry, M.P., Satellite studies of magnetospheric substorm on August 15, 1968, 9, Phenomenological model of substorms, *J. Geophys. Res.*, 78, 3131, 1973

Miller, F.D., Comet Tago-Sato-Kosaka 1969 IX : Tail Structure 25 December to 12 January 1970, *Icarus*, 37, 443-456, 1979.

Min, K., Okuda, H., and Sato, T., Numerical studies on magnetotail formation and driven reconnection, *J. Geophys. Res.*, 90, 4035, 1985.

Ness, N.F. and Donn, B.D., Concerning a New Theory of Type I Comet Tails, *Mem. Soc. Rpoy. Liege, Ser.* 5, 12, 141-144, 1965

Nha, I.-S., Korean Observation Records of Comets archived in Yonsei University, *Dong Bang Hak Ji*(in Korean), 34, 207-247, 1982.

Niedner, M.B., Jr., Interplanetary Gas. XXV Ⅱ. A Catalog of Disconnection Events in Cometary Plasma Tails *Astrophys. J. Suppl.*, 46, 141, 1981.

Niedner, M.B., Jr., and Brandt, J.C., Interplanetary Gas. XXⅢ. Plasma Tail Disconnection Events in Comets : Evidence for Magnetic Field Line Reconnection at Interplanetary Sector Boundaries?, *Astrophys. J.*, 223, 655, 1978.

Niedner, M.B., Jr. Schwingenschuh, K., Plasma-tail Activity at the time of the Vega Encounters, *Astrophys. Astrono.*, 187, 103-108, 1987.

Ogino, T., Walker, R.J., and Ashour-Abdalla, M., An MHD simulation of the interaction of the solar wind with the

outflowing plasma from a comet *Geophys, Res. Lett.*, 13, 929-932, 1986.

Ogino, T., Walker, R.J., and Ashour-Abdalla, M., A Three-Dimesional MHD Simulation of the solar Wind with Comet Halley *J. Geophys. Res.*, 93, 9568-9576, 1988.

Parker, E.N., Suprathermal Particle Generation in the Solar Corona, *Astrophys. J.*, 128, 664-676, 1958

Russell, C.T., Saunders, M.A., Phillips, J. L., and Fedder, J.A., Near-Tail Reconnection as the Cause of Cometary Tail Disconnections, *J. Geophys. Res.*, 91, 1417-1423, 1986.

Russell, C.T., G. Le, J.G. Luhmann and J. A. Fedder, A parametric study of the solar wind interaction with comets, in *Cometary Plasma Processes*, ed. by A.D. Johnstone, AGU, Washington, D.C., p. 153, 1991.

Schmidt, H.U., and R. Wegmann, MHD calculation for cometary plasma., *Comp. Phys. Comm.*, 19, 369, 1980.

Schmidt-Voigt, M., Time-dependent MHD simulation for cometary plasma, *Astrophys. Astronom.*, 210, 433-454, 1989.

Verigin, M.I., Axford, W.I., Gringauz, K.I., Richter, A.K., Acceleration of cometary plasma in the vicinity of comet Halley associated with an interplanetary magnetic field polarity change, *Geophys. Res. Lett.*, 14, 987-990, 1987

Wegmann, R., H.U. Schmidt, W.F. Huebner, and D.C. Boice, Cometary MHD and chemistry, *Astron, Astrophys.*, 187, 339, 1987.

Wurm, K. and Mammano, A., Contribution to the Kinematics of Type I Tails of Comets, *Astrophy. Space Science*, 18, 273-286, 1972.

Yeomans, D.K., *Comets*, Wiley, New York, 1991.

Yi, Y. and J.C. Brandt, A Preliminary 3D MHD Simulation of Cometary Plasma Tail Dynamics, *EOS Trans.*, 73, 444, 1992.

Yi, Y., F.M. Caputo, and J.C. Brandt, Disconnection Events(DEs) and Sector Boundaries : The Evidence from Comet Halley 1985-1986, *Planet. Space Sci.*, (in press), 1994.